



Identification of IFN-Induced Transmembrane Protein 1 With Prognostic Value in Pancreatic Cancer Using Network Module-Based Analysis

Lingyun Wu^{1†}, Xinli Zhu^{1†}, Danfang Yan¹, Mengmeng Tang², Chiyuan Ma^{3*†} and Senxiang Yan^{1*†}

¹ Department of Radiation Oncology, The First Affiliated Hospital, Zhejiang University School of Medicine, Hangzhou, China,

² Department of Pathology, The First Affiliated Hospital, Zhejiang University School of Medicine, Hangzhou, China,

³ Department of Orthopedic Surgery, The Second Affiliated Hospital, Zhejiang University School of Medicine, Hangzhou, China

OPEN ACCESS

Edited by:

Xiangqian Guo,
Henan University, China

Reviewed by:

Jiateng Zhong,
Xinxiang Medical University, China
Liang Chen,
Wuhan University, China
Guosen Zhang,
Henan University, China

*Correspondence:

Senxiang Yan
yansenxiang@zju.edu.cn
Chiyuan Ma
machiyuan@zju.edu.cn

[†]These authors have contributed
equally to this work

Specialty section:

This article was submitted to
Cancer Genetics,
a section of the journal
Frontiers in Oncology

Received: 07 November 2020

Accepted: 08 February 2021

Published: 22 March 2021

Citation:

Wu L, Zhu X, Yan D, Tang M, Ma C
and Yan S (2021) Identification of
IFN-Induced Transmembrane Protein
1 With Prognostic Value in Pancreatic
Cancer Using Network Module-Based
Analysis. *Front. Oncol.* 11:626883.
doi: 10.3389/fonc.2021.626883

Despite improvements reported in diagnosis and treatments in recent decades, pancreatic cancer is still characterized by poor prognosis and low survival rate among solid tumors. Intensive interests have grown in exploring novel predictive biomarkers, aiming to enhance the efficiency in early detection and treatment prognosis. In this study, we identified the differentially expressed genes (DEGs) in pancreatic cancer by analyzing five gene expression profiles and established the functional modules according to the functional interaction (FI) network between the DEGs. A significant upregulation of the selected DEG, interferon (IFN)-induced transmembrane protein 1 (IFITM1), was evaluated in several bioinformatics online tools and verified with immunohistochemistry staining from samples of 90 patients with pancreatic cancer. Prognostic data showed that high expression of IFITM1 associated with poor survival, and multivariate Cox regression analysis showed IFITM1 was one of the independent prognostic factors for overall survival. Meanwhile, significant correlations of the expression of IFITM1 and the infiltration of immune cells were found by TIMER. Furthermore, a higher level of IFITM1 was assessed in pancreatic cancer cell lines compared to normal human pancreatic duct epithelial cells, and silencing IFITM1 in tumor cells remarkably inhibited cancer tumorigenicity. Collectively, our findings suggested that IFITM1 might have promising utility for pancreatic cancer.

Keywords: IFITM1, IFN-induced transmembrane protein 1, pancreatic cancer, functional interaction network, prognostic biomarker, tissue microarray detection

INTRODUCTION

Pancreatic cancer is expected to be the second leading cause of cancer-related deaths in developed countries by 2030, and is characterized as highly invasive and metastatic as well as extremely resistant to chemo-radio-therapy (1). Despite some efforts made on adjuvant therapeutics recent years, the clinical mortality ratio remains elevated to date (2). The 5-year survival rate was reported <10% with an estimated 432,242 deaths occurring worldwide in 2018 (3). Because of this poor

prognosis, better identification of clinical biomarkers useful for making therapeutic decisions and developing targets for innovative drugs are urgently needed in this complex and heterogeneous mutational landscape.

The human interferon (IFN)-induced transmembrane protein 1 (IFITM1), also named Leu13 or CD225, is a 17-kDa cell-surface membrane protein in the IFN-stimulated genes (ISGs) protein family along with IFITM2 and IFITM3. Since it was first discovered in neuroblastoma cells in 1984, it has been identified participating in various biological processes (BPs) including cell proliferation and adhesion and being important in immunity and antiviral activities (4, 5). Particularly, more and more studies have confirmed that IFITM1 is overexpressed in numerous human cancers during the last decade, such as lung, gastric, colorectal, and ovarian cancers (6–9). Furthermore, the positive IFITM1 expression was illustrated in correlations with poorer prognosis in diverse tumors (10, 11). Hence, it is very likely that IFITM1 may also hold hitherto undiscovered value in pancreatic cancer and might be further associated with prognosis of patients with pancreatic cancer.

In this study, we investigated gene expression profiles from Gene Expression Omnibus (GEO) repository to screen out common DEGs between pancreatic cancer and normal pancreatic tissues and analyzed them by establishing a protein functional interaction (FI) network. Functional network-based modules were constructed, and biological pathways were analyzed afterward. It was confirmed that IFITM1 played a vital role in pancreatic cancer by analyzing the clinical and pathological characteristics of 90 patients with pancreatic cancer and their survival rate as well as by verifying through several bioinformatics online tools. Our study suggested that IFITM1 may have promising clinical utility for prognostic stratification, and combining IFITM1 expression profiles systematically with clinical characteristics of patients is promising to be effective for developing treatment.

MATERIALS AND METHODS

Research Tools

(1) BRB-Array Tools (version 4.6.0; <http://linus.nci.nih.gov/BRB-ArrayTools.html>) were used to analyze the DEGs (12); (2) the Cytoscape software (version 3.7.1; <http://www.cytoscape.org>) was applied to construct FI network and the network-based functional modules; (3) the FunRich (version 3.1.3; <http://www.funrich.org>) was used to construct biological pathways (13); (4) the Omicshare online database (<https://www.Omicshare.com/>), a commercial database based on the Database for Annotation, Visualization, and Integrated Discovery (DAVID), was used for the visual analysis of Gene Ontology (GO), and Kyoto

Encyclopedia of Genes and Genomes (KEGG) was used for enrichment analysis (14); (5) the MultiExperiment Viewer (MeV) application (version 4.9.0; <http://mev.tm4.org/>) was used to generate the heat map; and (6) some bioinformatics online tools such as the Oncomine database (<https://www.oncomine.org/>), the Human Protein Atlas (<https://www.proteinatlas.org/>), the interactive web application Gene Expression Profiling Interactive Analysis (GEPIA) (<https://www.gepia.cancer-pku.cn>), and the TIMER database (<https://cistrome.shinyapps.io/timer/>) were used. A detailed flowchart of identifying the targeted genes associated with pancreatic cancer is shown in **Figure 1**.

Patient Samples Preparation

Between 2004 and 2008, a total of 90 human pancreatic cancer specimens were collected from the Taizhou People's Hospital of China for tissue microarray (TMA) detection, 60 of which were paired nonmalignant tissue. All the specimens were stored at the Biobank Center of National Engineering Center for Biochips at Alenabio and Shanghai Outdo Biotech Company, China. All the patients received no preoperative anticancer treatment or postoperative adjuvant chemo-radio-therapy. Histological differentiation grade and disease stages were classified according to the American Joint Committee on Cancer (AJCC) TNM Classification (7th Edition). The follow-up time was recorded from the date of the surgery to the date of death or last visit to the clinic. The use of pancreatic cancer samples and clinical data were reviewed and approved by the Ethical Committees of the National Engineering Center for Biochips at Shanghai along with the Taizhou People's Hospital. Informed consent was written in accordance with the Declaration of Helsinki from all participants.

Microarray Data

To investigate biological characteristics of genes differently expressed between pancreatic cancer and normal pancreatic tissues, five data sets were retrieved from National Center for Biotechnology Information (NCBI)-GEO (<http://www.ncbi.nlm.nih.gov/geo/>) for the analysis, including GSE101448 (18 with pancreatic tumor and 13 non-tumor pancreatic tissue samples), GSE62165 (118 pancreatic tumor samples and 13 control samples), GSE62452 (69 pancreatic tumor and adjacent non-tumor tissues), GSE41372 (matched pancreatic ductal adenocarcinoma samples from 15 patients), and GSE28735 (45 matching pairs of pancreatic tumor and adjacent non-tumor tissues). NCBI-GEO is a public repository containing an initial database of 1,325 biologically defined gene profiles and was developed to help in the analysis and interpretation of the long lists of genes produced from microarray-based experiments. The details of the series data are listed in **Table 1**.

Initial Identification of DEGs

As microarray batch effects appear to be the major contributors to the differential expression, SangerBox online tool (<http://sangerbox.com/>) was used to eliminate them before taken into account (15). Later, data were imported into the BRB-Array Tools to identify the DEGs between pancreatic tumor and normal pancreatic tissues. The Affymetrix platform (Santa Clara,

Abbreviations: IFN, interferon; IFITM1, IFN-induced transmembrane protein 1; ISGs, IFN-stimulated genes; GEO, Gene Expression Omnibus; DEGs, differentially expressed genes; FI, functional interaction; GO, Gene Ontology; KEGG, Kyoto Encyclopedia of Genes and Genomes; FDR, false discovery rate; TCGA, the Cancer Genome Atlas; IHC, immunohistochemical; MCL, Markov cluster algorithm; NSCLC, non-small cell lung cancer; TMA, tissue microarray; BP, biological process; MF, molecular function; HNSCC, head and neck squamous cell carcinoma; OS, overall survival.

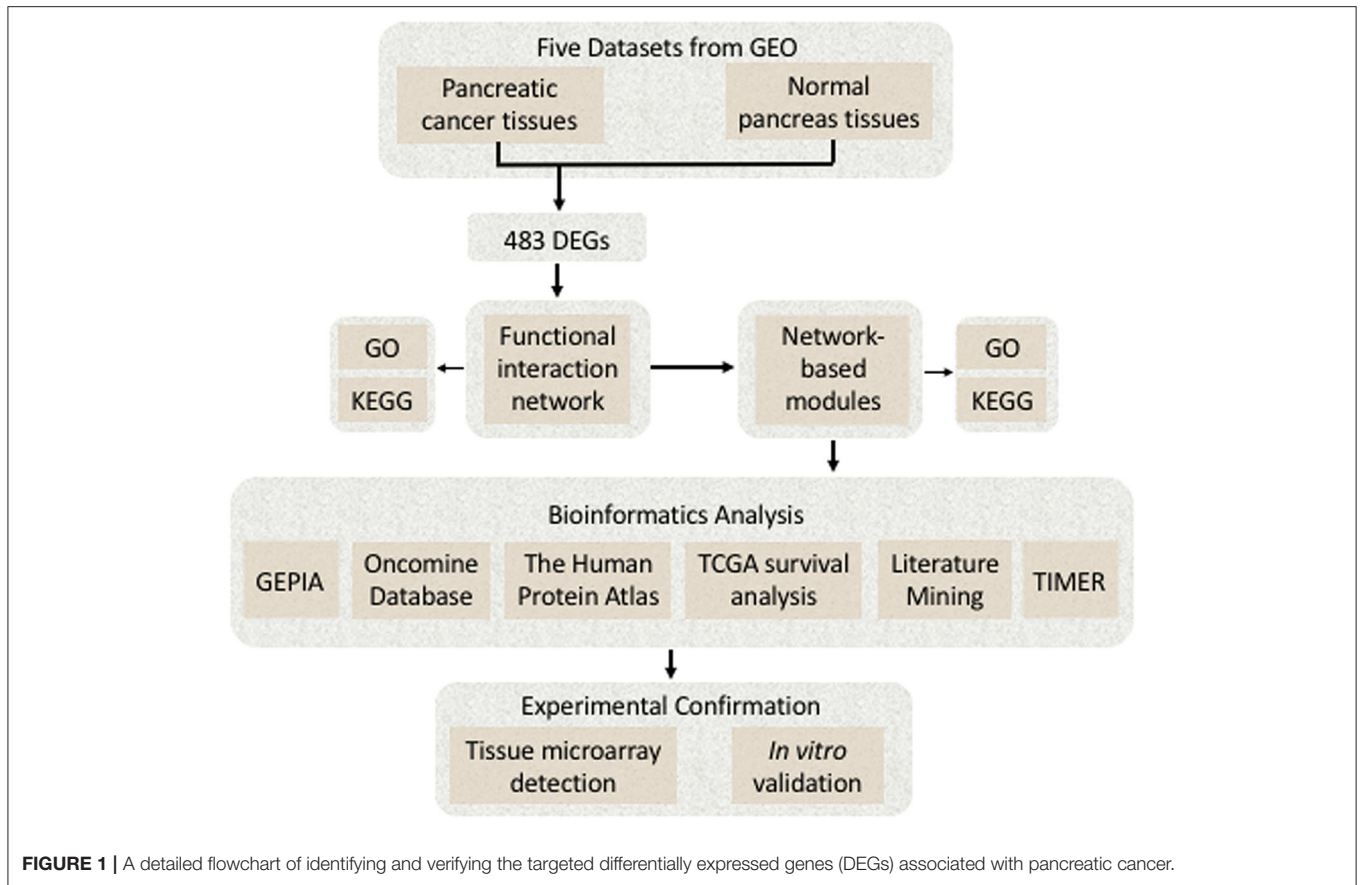


TABLE 1 | Detailed information of the five GEO data sets in the study.

| Series | Organism | Study type | Platform | Country | Samples |
|-----------|---------------------|-------------------------------|--|---------|---|
| GSE101448 | <i>Homo sapiens</i> | Expression profiling by array | GPL10558 Illumina HumanHT-12 V4.0 expression beadchip | Germany | 18 with pancreatic tumor and 13 non-tumor pancreatic tissue samples |
| GSE62165 | <i>Homo sapiens</i> | Expression profiling by array | GPL13667 [HG-U219] Affymetrix Human Genome U219 Array | Belgium | 118 surgically resected PDAC and 13 control samples |
| GSE62452 | <i>Homo sapiens</i> | Expression profiling by array | GPL6244 [HuGene-1_0-st] Affymetrix Human Gene 1.0 ST Array [transcript (gene) version] | USA | 69 pancreatic tumors and 61 adjacent non-tumor tissue from patients with pancreatic ductal adenocarcinoma |
| GSE41372 | <i>Homo sapiens</i> | Expression profiling by array | GPL6244 [HuGene-1_0-st] Affymetrix Human Gene 1.0 ST Array [transcript (gene) version] | Italy | 15 paired pancreatic tumor and adjacent non-tumor tissues |
| GSE28735 | <i>Homo sapiens</i> | Expression profiling by array | GPL6244 [HuGene-1_0-st] Affymetrix Human Gene 1.0 ST Array [transcript (gene) version] | USA | 45 matching pairs of pancreatic tumor and adjacent non-tumor tissues from 45 patients with pancreatic ductal adenocarcinoma |

California, USA) was applied for data set and gene annotation. The probes were filtered when some gene expression data were missing. The Bioinformatics and Evolutionary Genomics

web tool (<http://bioinformatics.psb.ugent.be/webtools/Venn/>) was depicted graphically in the form of Venn diagram to detect the common DEGs among the five data sets.

Establishment of FI Network

The Reactome pathway database (version 7.2.0; <http://www.reactome.org>) was applied to analyze the pathway enrichment for the sets of genes, investigate the functional relationships of the genes, and visualize the outcomes with diagrams that can be manually generated (16). Over 60% of human proteins were covered to help construct the Reactome FI network. The pairwise interaction information was uploaded into Cytoscape software (<http://www.cytoscape.org>) to establish the FI network (17). A false discovery rate (FDR) <0.05 was accepted as the cutoff criterion.

Construction of the FI Network-Based Functional Modules

To construct the FI network-based module analysis, the Microarray Data Analysis bioinformatics tool installed in the ReactomeFIViz was applied (18). After uploading the text file containing gene expression data, correlations between genes in the FI-network were analyzed. The Markov Cluster algorithm (MCL) was used to achieve the functional modules with a selected module size. In order to supervise the size of the modules, we inputted 5.0 for the inflation coefficient (19). MCL modules in size of three or more were applied, and the average Pearson's correlation coefficient was ≥ 0.25 . Six different colors were used to label the nodes in six different network modules. Module size ≥ 7 and fluorodeoxyglucose (FDG) <0.05 were used as cutoffs for the KEGG pathway and GO term enrichment analysis of the modules in a separate manner.

Preliminary Validation of the Selected Gene

The Human Protein Atlas (<http://www.proteinatlas.org>) presented an expression map of human protein across 20 cancer types and 44 normal human tissues. It measured the RNA level as well as used antibody profiling to precisely localize the corresponding proteins (20). With the Human Protein Atlas (<http://www.proteinatlas.org>), we detected the IFITM1 protein expression in both pancreatic cancer and normal pancreatic tissues. Oncomine microarray database (<http://www.oncomine.org>) is a cancer microarray database as well as an online data-mining platform which contains 65 gene expression data sets comprising nearly 48 million gene expression measurements from over 4,700 microarray experiments (21). With the Oncomine online tool (<http://www.oncomine.org>), we explore the expression of IFITM1 in pancreatic cancer and normal pancreatic tissues across eight different data sets.

Validation of IFITM1 With the Cancer Genome Atlas

Gene Expression Profiling Interactive Analysis (<http://gepia.cancer-pku.cn/>) is an online server, containing more than 8,000 normal and 9,000 tumor samples, providing interactive and customizable functions based on the Cancer Genome Atlas (TCGA) and Genotype-Tissue Expression (GTEx) database (22). Boxplot with jitter was applied to compare the expression level of IFITM1 mRNA in pancreatic cancer and paired normal pancreatic tissues. To validate the expression of IFITM1 correlating with survivals and pathological stages of patients with

pancreatic cancer, the database was searched to obtain Kaplan-Meier survival curves and violin plots. The requested mRNA expressions above or below the median classified the patients into both high and low expression groups. The log-rank *p*-value and hazard ratio (HR) with 95% CIs were calculated and displayed on the website. A value of *p* < 0.05 was considered statistically significant.

Immunohistochemical Staining

To analyze the IFITM1 expression by immunohistochemical (IHC) staining experiment, 90 patients with pancreatic cancer were included in the TMA analysis. Sample slides were dried for adherence and deparaffinized in xylene for decreasing ethanol concentrations. The tissue sections were marked and incubated with rabbit anti-IFITM1 diluted 1:1,500 (ab224063, Abcam, Cambridge, UK) at 4°C overnight. The percentage of the IHC staining and the staining intensity were assessed and recorded by two pathologists from the department of pathology, who were both blinded to the features of patients. The H-scores ranged from 0 to 100, where 100 represented 100% of regions with strong intensity. The H-scores were dichotomized by the cutoff and the median value for the statistical analysis.

Cell Lines Culture and Short Hairpin RNA Lentiviral Transduction

Three human pancreatic cancer cell lines, PanC-1, BxPc-3, and SW1990, and one normal pancreatic cell line, HPDE6-C7, were used in the study. The panC-1 and BxPc-3 cells were purchased from the Cell Bank of Shanghai Institute of Biochemistry and Cell Biology (Shanghai, China), and the others were purchased from the American Type Culture Collection (ATCC, Manassas, VA, USA). The panC-1 and HPDE6-C7 cells were cultured in Dulbecco's modified Eagle's medium (DMEM) (Gibco, Brooklyn, NY, USA), and the BxPc-3 and SW1990 cells were cultured in Roswell Park Memorial Institute Medium (RPMI) 1640 (Gibco, Brooklyn, NY, USA) with both cultures supplemented with 10% fetal bovine serum (FBS; Gibco, Brooklyn, NY, USA) and 100 U penicillin/streptomycin (Gibco, Brooklyn, NY, USA) in a humid atmosphere containing 5% CO₂ at 37°C. Short-tandem repeat (STR) profiles were authenticated to ensure the quality of the cell lines. All of the cells were passaged by standard cell culture techniques.

Two lentivirus-derived short hairpin RNAs (shRNAs) against IFITM1 were designed by Biolink Biotechnology Co. Ltd (Beijing, China) to silence the IFITM1 mRNA expression (the targeted sequences as follows: IFITM1 shRNA-1, 5'-CCTCATGACCATTGGATTCAT-3'; IFITM1 shRNA-2, 5'-CCTGTTCAACACCCTCTTCTT-3'). The procedure of transducing pancreatic cancer lines with shRNA lentiviral transduction was described in detail previously (23).

Cell Viability Assay

Cells in logarithmic growth phase were seeded in 96-well Falcon Petri dishes (3,000 cells/well) the day before the assays were performed. The cell viability was assessed using a Cell Counting Kit (Dojindo, Kumamoto, Japan) based on sensitive colorimetric assays with the absorbance measured

at 450 nm (OD 450 nm), according to the instructions of the manufacturer. The results were confirmed with three independent experiments.

Quantitative Real-Time PCR Analysis

To extract total RNA, cells were lysed with the TRIzol Reagent (Invitrogen Corporation, Carlsbad, CA, USA) and reversed

into complementary DNA (cDNA) with the QuantiTect Reverse Transcription Kit (TaKaRa, Dalian, China). The sequences of the designed primers used for the real-time PCR (qRT-PCR) experiments were as follows: IFITM1 forward, 5'-AGCCAGAAGATGCACAAGGA-3' and reverse, 5'-GATCACGGTGGACCTTGGAA-3'; GAPDH forward, 5'- GAAGGTCGGTGTGAACGGATTG-3' and reverse,

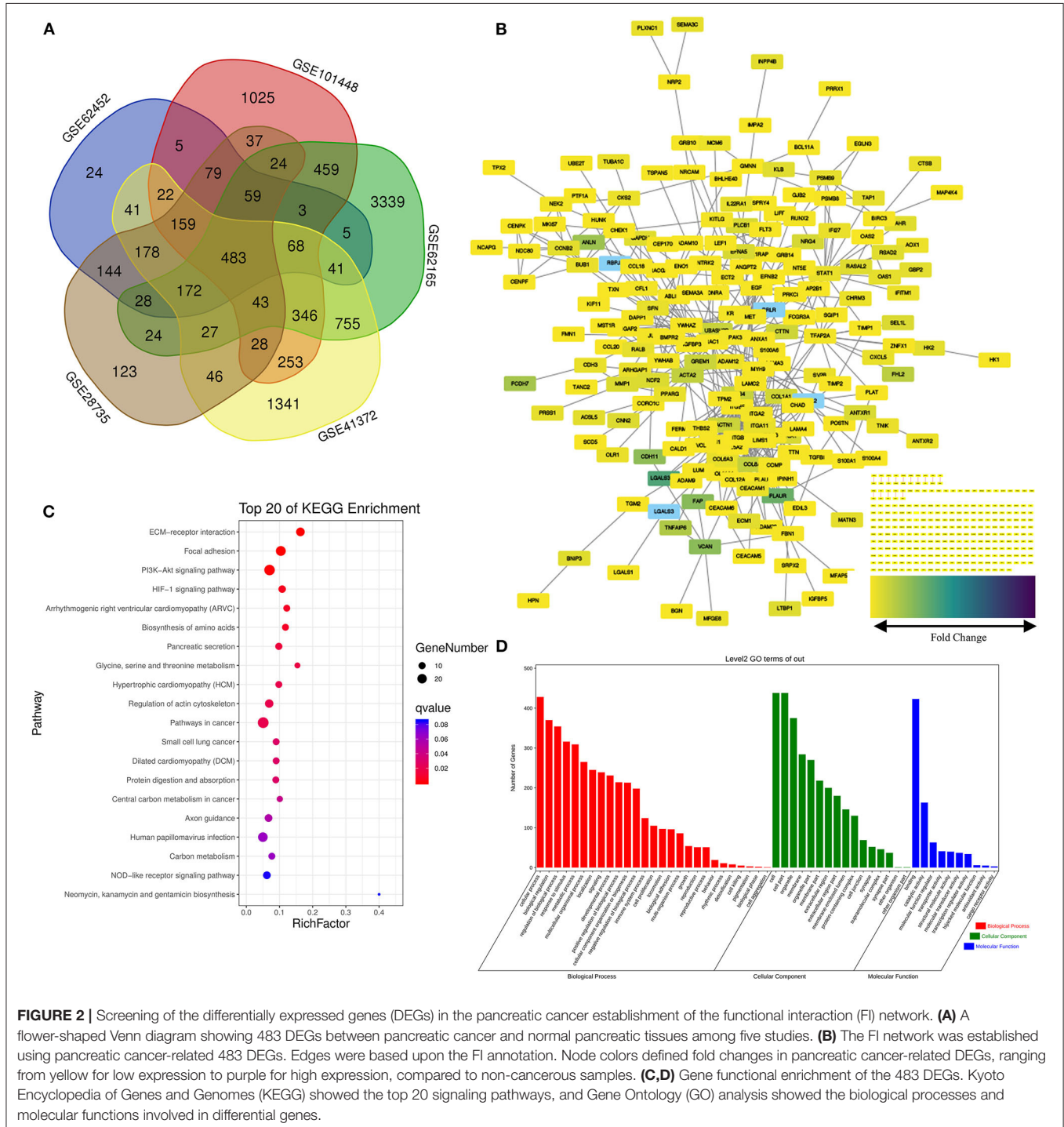


FIGURE 2 | Screening of the differentially expressed genes (DEGs) in the pancreatic cancer establishment of the functional interaction (FI) network. **(A)** A flower-shaped Venn diagram showing 483 DEGs between pancreatic cancer and normal pancreatic tissues among five studies. **(B)** The FI network was established using pancreatic cancer-related 483 DEGs. Edges were based upon the FI annotation. Node colors defined fold changes in pancreatic cancer-related DEGs, ranging from yellow for low expression to purple for high expression, compared to non-cancerous samples. **(C,D)** Gene functional enrichment of the 483 DEGs. Kyoto Encyclopedia of Genes and Genomes (KEGG) showed the top 20 signaling pathways, and Gene Ontology (GO) analysis showed the biological processes and molecular functions involved in differential genes.

5'- CATGTAGACCATGTAGTTGAGGTCA-3' (Sangon, Shanghai, China).

Western Blot Analysis

Radioimmunoprecipitation assay (RIPA; Invitrogen Corporation, Carlsbad, CA, USA) was added to protease, and phosphatase inhibitors were used to gain total protein samples. The proteins were separated by the sodium dodecyl sulfate-polyacrylamide gel electrophoresis (SDS-PAGE) gel (Bio-Rad, Hercules, CA, USA) and transferred to the polyvinylidene fluoride (PVDF) membrane (Sigma Chemical Corporation, St. Louis, MO, USA). The membranes were blocked for 1 h and then incubated overnight with primary antibodies against IFITM1 and β -actin (Abcam, Cambridge, UK), followed by the horseradish peroxidase (HRP)-linked secondary antibodies. SuperSignal West Femto Maximum Sensitivity Substrate (Thermo Fisher Scientific, Waltham, MA, USA) was used to detect the probed proteins.

Wound Healing Assay

The cells were seeded in 48-well Falcon (Thermo Fisher Scientific Inc. Waltham, Massachusetts, USA) Petri dishes. Once 80–90% confluence was reached, a 200- μ l sterile plastic pipette tip was used to make a single wound by gently scratching in every well. Cell debris was removed using phosphate-buffered saline and refreshed with serum-free medium immediately. Cells that extended the borders of the wound were photographed and quantified in three randomly selected regions per well.

Colony Formation Assay

The cells in the logarithmic growth phase were seeded in 6-well Falcon Petri dishes (500 cells/well) and incubated for 7–14 days. The medium was refreshed every 3 days. The colonies were fixed with 70% ethanol and stained with crystal violet (0.5% w/v). The cell colonies containing at least 50 cells were photographed and quantified. The results were presented as mean \pm SD for three independent experiments.

Statistical Analysis

Statistical analyses were performed using SPSS 23.0 (SPSS Inc., Chicago, IL, USA) and Prism 8 (GraphPad Software, San Diego, CA, USA). Correlations between protein expression and clinicopathological features in patients with pancreatic cancer were analyzed by the χ^2 -test. Overall survival (OS) was evaluated using the Kaplan–Meier method and the log-rank test. A Cox proportional hazards regression model was used to assess the univariate and multivariate analyses. The Enter method was used to select the independent variables in the multivariate analysis.

RESULTS

Screening of DEGs

Five data sets from GEO containing gene expression profiles of pancreatic cancer as well as normal pancreas samples were downloaded for microarray analysis. The random variance mode method along with the paired *t*-test was applied for the differential expression calculation. Considering the criteria of $|\log_2(\text{Fold change})| > 1$ adjusted $p < 0.05$, 483 DEGs

were obtained (Figure 2A). Of those, 231 DEGs were identified upregulated and 252 downregulated (Supplementary Table 1).

Establishment of the Pancreatic Cancer-Related FI Network

Functional interaction data derived from the Human Protein Reference Database (<http://www.hprd.org/>) (24), BioGrid (<https://thebiogrid.org/>) (25), I2D (<http://ophid.utoronto.ca/>) (26), IntACT (<https://www.ebi.ac.uk/intact/>) (27), MINT (<https://www.ebi.ac.uk/intact/>) (28), the Database of Interacting Proteins (<http://dip.doe-mbi.ucla.edu>) (29) as well as multiple high-throughput assays (30). We established the FI network by mapping the pancreatic cancer-related DEGs to the FIs data. Of 245 isolated nodes, 227 in eight clusters were identified with an effective mean degree of 2.20 (Figure 2B). The connectivity of a node represents the number of its neighbors, and the neighborhood connectivity represents the average connectivity of all neighbors of the selected node. Under the criteria of neighborhood connectivity ≥ 20 and the shortest path length ≥ 3.5 for non-single modules, eight genes (*EDIL3*, *RSAD2*, *AHR*, *GBP2*, *IFITM1*, *AOX1*, *KIF11*, and *CEP170*) among all the nodes in the FI network were filtered out (Supplementary Table 2).

Functions Analysis of the FI Network

To gain insights into the role of the putative targets involved in various BPs and molecular functions (MFs), the preliminary GO function and KEGG pathway analysis were performed using the OmicShare online database. As expected, among the top 20 KEGG pathways, extracellular matrix (ECM)–receptor interaction, pancreatic secretion, and pathways in cancer had significant relations to tumorigenesis and progression of pancreatic cancer (Figure 2C; for details see Supplementary Table 3). Among the most highly enriched functions in the BP category, cell process, biological regulation, and regulation of BP were found associated with the

TABLE 2 | Genes analyzed in six modules in the FI network.

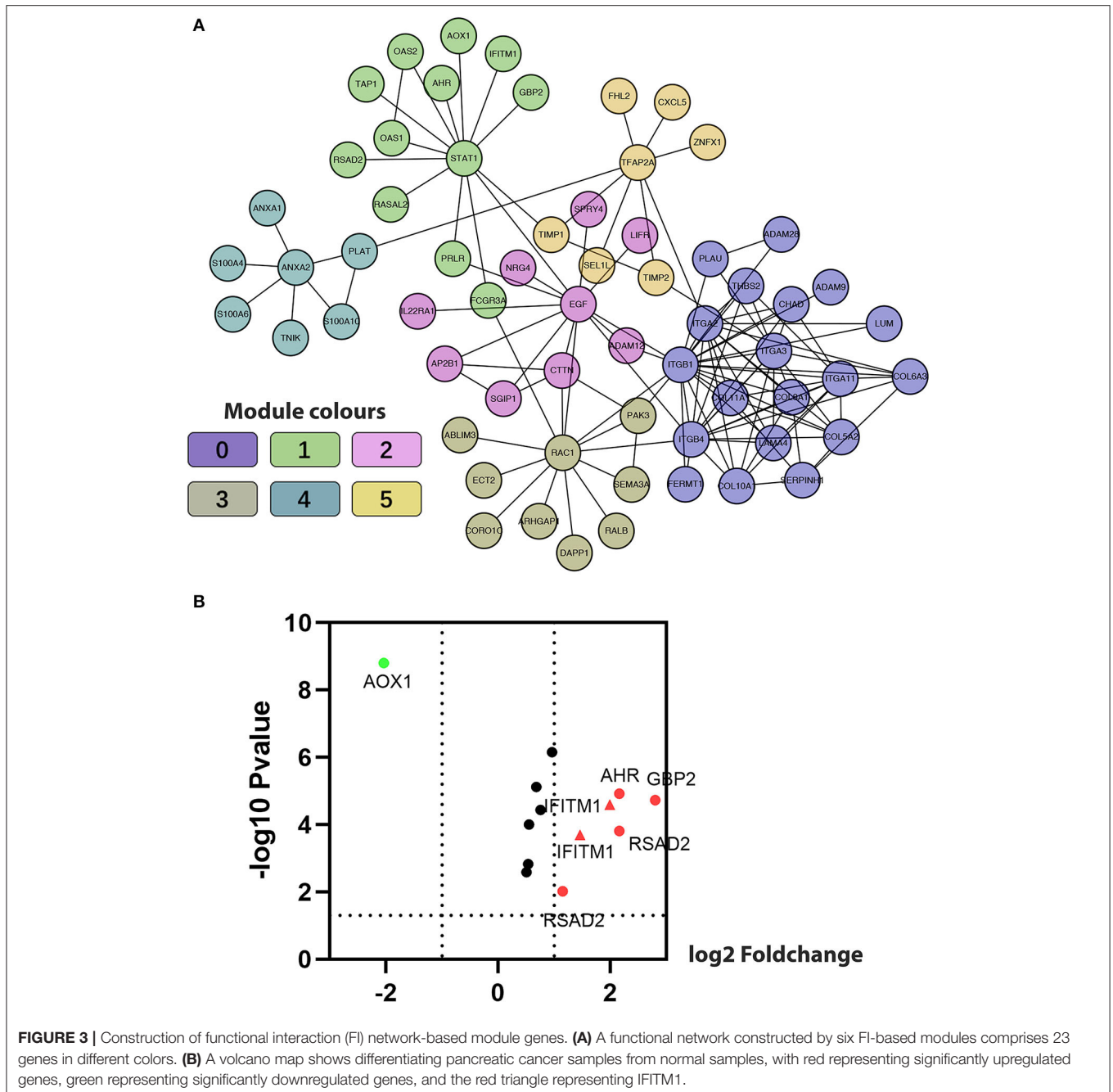
| Module number | Number of genes | Average correlation | Gene set |
|---------------|-----------------|---------------------|--|
| 0 | 19 | 0.9927 | ADAM28, ADAM9, CHAD, COL10A1, COL11A1, COL5A2, COL6A3, COL8A1, FERMT1, ITGA11, ITGA2, ITGA3, ITGB1, ITGB4, LAMA4, LUM, PLAU, SERPINH1, THBS2 |
| 1 | 12 | 1.0000 | AHR, AOX1, FCGR3A, GBP2, IFITM1, OAS1, OAS2, PRLR, RASAL2, RSAD2, STAT1, TAP1 |
| 2 | 9 | 0.9615 | ADAM12, AP2B1, CTTN, EGF, IL22RA1, LIFR, NRG4, SGIP1, SPRY4 |
| 3 | 9 | 0.8365 | ABLIM3, ARHGAP1, CORO1C, DAPP1, ECT2, PAK3, RAC1, RALB, SEMA3A |
| 4 | 7 | 0.9739 | ANXA1, ANXA2, PLAT, S100A10, S100A4, S100A6, TNIK |
| 5 | 7 | 0.7790 | CXCL5, FHL2, SEL1L, TFAP2A, TIMP1, TIMP2, ZNFX1 |

tumorigenesis and progression of pancreatic cancer. Meanwhile, cell, cell part, organelle, and membrane were top enriched items in the cellular component (CC) category. In the MF category, the DEGs were mainly enriched in binding activities (Figure 2D; for details see Supplementary Tables 4–6).

Identification of FI Network-Based Functional Modules

The Markov Cluster algorithm (MCL) was applied for the network-based module-clustering algorithm, and the absolute

value of the Pearson’s correlation coefficient of the interacting genes was used to weigh each correlation edge. A total of 6 modules involving 63 genes were obtained, ranging from 7 to 19 genes per module (Table 2, Figure 3A). Later, GO function and pathway analyses were performed on the six network-based functional modules. Through enrichment analysis (Supplementary Table 7), we identified that Module 0 containing 19 genes was in relation to the classical cell–cell adhesion process. Module 1 was of the highest average correlation and was related to the classical cancer signaling pathway in the KEGG and IFN-gamma pathway in NCI-PID. Module 2



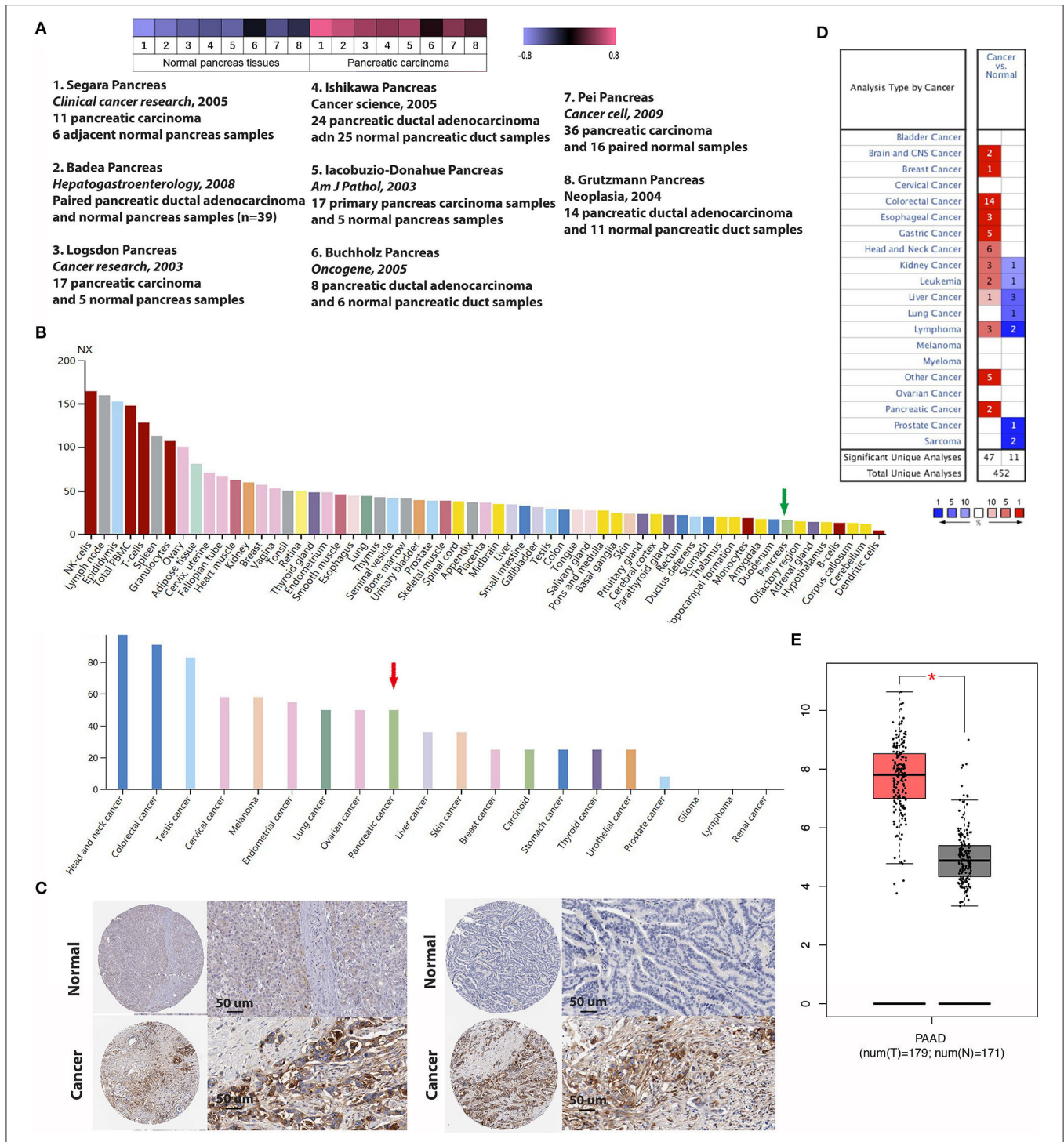
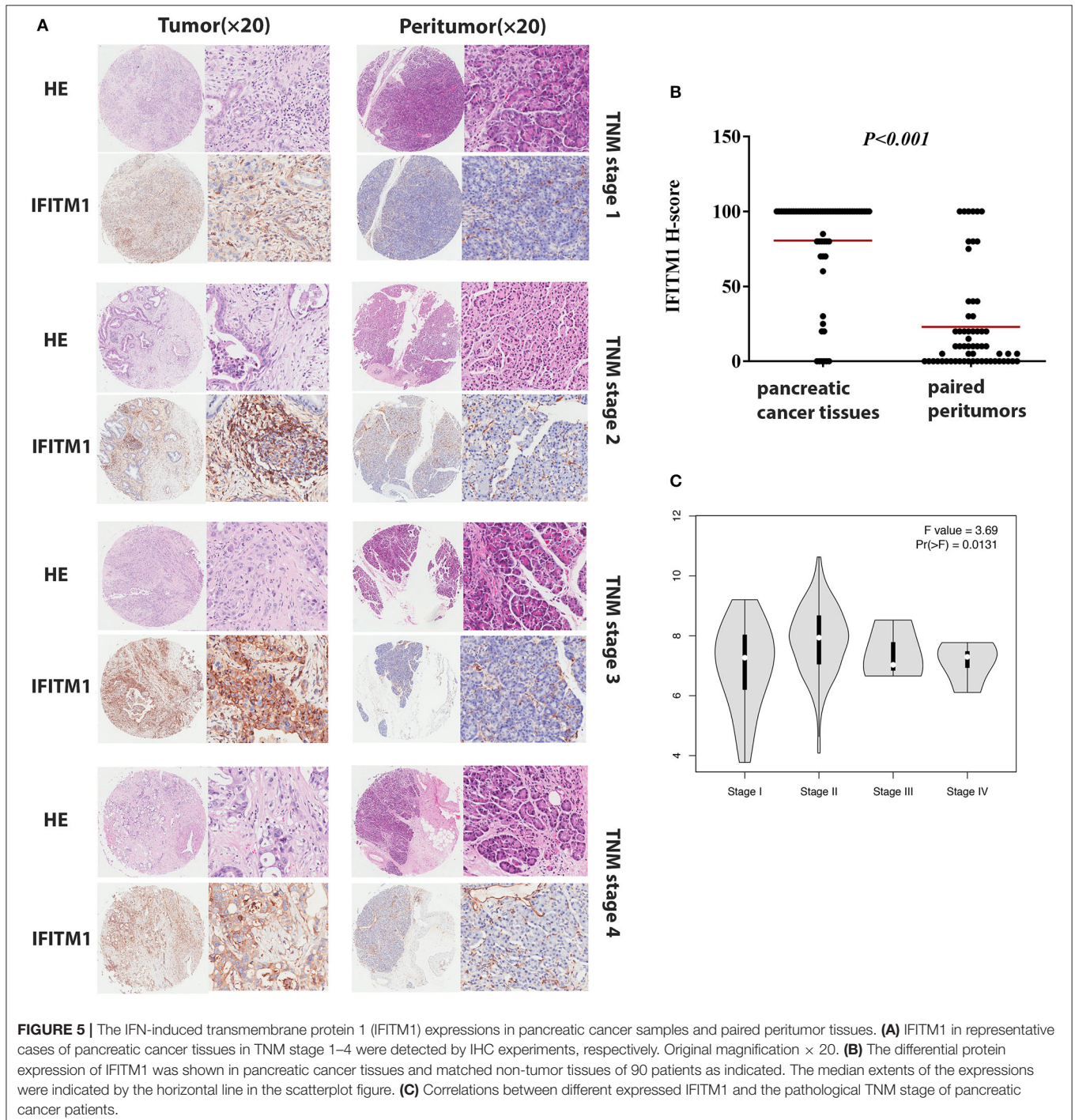


FIGURE 4 | The expression of IFN-induced transmembrane protein 1 (IFITM1) between pancreatic cancer and normal pancreas samples. **(A)** Heat map of IFITM1 associated with pancreatic cancer among eight studies. **(B,C)** An overview of IFITM1 levels in pancreatic tumors and normal pancreatic tissues and immunohistochemical analysis of IFITM1 expression in pancreatic cancer and normal pancreatic tissues. Data were derived from the Human Protein Atlas database. **(B)** The green and the red arrows represent normal pancreatic tissue and pancreatic cancer, respectively. **(C)** Top: Protein levels of IFITM1 in normal tissue (staining: negative; intensity: negative; quantity: none); bottom: Protein levels of IFITM1 in pancreatic cancer tissue (staining: high; intensity: strong; quantity: >75%). **(D)** mRNA levels of IFITM1 in 20 types of cancers vs. normal tissues. The figure represented the number of data sets involving statistically significant upregulated (dark) as well as downregulated (light) expression of IFITM1. **(E)** The box plot shows the expression profile of the IFITM1 based on GEPIA. The red node represents pancreatic cancer, and the gray node represents normal samples. * $p < 0.05$.

was found related to cell motility and proliferation in KEGG and Module 3 to cell migration and cytoskeleton. Fibro-relevant families in Reactome were enriched in Module 4. Meanwhile, the enrichment of GO term was also analyzed. The calculation results showed that the GO functions of six modules complied with the pathway annotations (**Supplementary Tables 8–10**).

Five genes (*IFITM1*, *AHR*, *AOX1*, *GBP2*, and *RSAD2*) common to both Module 1, with an average correlation equal to 1.00, and the set of previously selected eight genes

were selected for the volcano plot analysis of the five GEO data sets (**Figure 3B**, *IFITM1* marker in the red triangle). Through comprehensive literature searching, studies relative to *AHR* and pancreatic cancer have been taken, but not enough background data was found about *AOX1*, *GBP2*, and *RSAD2* (31). Combining the results from the functional analysis of the FI network and literature mining, we were interested to see if *IFITM1* could be a potential biomarker in pancreatic cancer.



Aberrant Expression of IFITM1 in Pancreatic Cancer

First, we used the Oncomine database to explore the transcriptional level of IFITM1 in pancreatic cancer and normal pancreatic tissues (**Figure 4D**). Based on the data from the Oncomine database, the transcriptional level of IFITM1 was significantly elevated in pancreatic cancer tissue vs. normal pancreatic tissue. Same results can also be seen in colorectal, esophageal, gastric, liver, and many other cancer types. Eight studies reported from 2003 to 2009 were filtered out with the screening condition of “IFITM1; Cancer vs. Normal Analysis; Cancer Type: Pancreatic Cancer” and assessed with a heat map analysis (**Figure 4A**). Segara et al. (32) found that the level of IFITM1 in pancreatic cancer was significantly increased compared to adjacent normal pancreas samples, with a fold change of 5.521 and a *p*-value of 6.78E-7. The same results were also reported by Badea et al. (33) (fold change of 3.065 and *p*-value of 8.21E-9), Logsdon et al. (34) (fold change of 4.104 and *p*-value of 1.14E-4), Ishikawa et al. (35) (fold change

of 2.350 and *p*-value 0.008), and Iacobuzio-Donahue et al. (36) (fold change of 2.855 and *p*-value of 0.005), respectively. While Buchholz et al. (37) and Grutzmann et al. (38) found no significant upregulation in pancreatic cancer with *p*-values of 0.412 and 0.231, respectively. Recently, Pei et al. (39) studied 36 samples of pancreatic carcinoma and 16 paired normal samples, and statistical significance was reported with a fold change of 2.304 and a *p*-value of 0.002. Meanwhile, we found the protein expression of IFITM1 with the help of the Human Protein Atlas, and the positively strong level was also found in pancreatic cancer specimens compared with normal tissues (**Figures 4B,C**). Furthermore, the GEPIA online tool (<https://www.gepia.cancer-pku.cn>) was also used to validate the differential mRNA expression analysis of IFITM1 in pancreatic cancer and normal tissues (**Figure 4E**).

Immunohistochemical experiments were applied to validate IFITM1 expression in 90 patients with pancreatic cancer. Representative IHC-stained images showed that IFITM1 is mainly located in the cell membrane of the pancreatic cancer

TABLE 3 | Relationship between the expression of IFITM1 and clinical characteristics of 90 patients with pancreatic cancer.

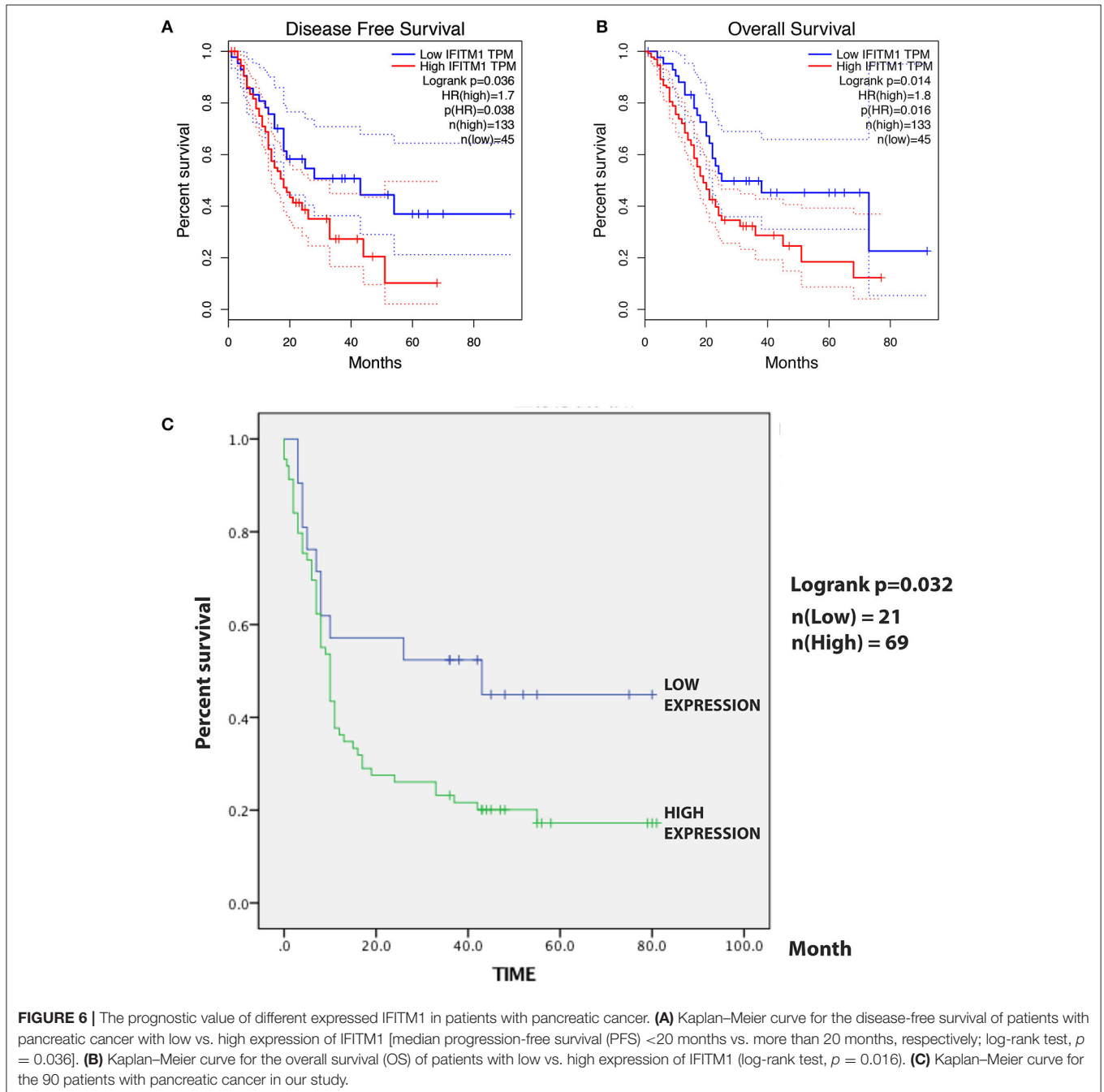
| Parameter | Patients | | IFITM1 expression | | |
|----------------------------|----------|------------|-------------------|------|-----------------|
| | Number | Percentage | Low | High | <i>p</i> -value |
| Gender | | | | | 0.808 |
| Male | 58 | 64.44 | 14 | 44 | |
| Female | 32 | 35.56 | 7 | 25 | |
| Age at diagnosis (year) | | | | | 0.944 |
| ≤65 | 54 | 60.00 | 13 | 41 | |
| >65 | 36 | 40.00 | 9 | 27 | |
| Tumor size (cm) | | | | | 0.839 |
| ≤4.5 | 54 | 60.00 | 13 | 41 | |
| >4.5 | 36 | 40.00 | 8 | 28 | |
| Histologic differentiation | | | | | 0.032 |
| Well | 9 | 10.00 | 4 | 5 | |
| Moderate | 48 | 53.55 | 14 | 34 | |
| Poor | 33 | 36.67 | 3 | 30 | |
| TNM stage | | | | | 0.044 |
| 1 | 3 | 3.33 | 2 | 1 | |
| 2 | 66 | 72.22 | 12 | 54 | |
| 3 | 18 | 21.11 | 7 | 11 | |
| 4 | 3 | 3.33 | 1 | 2 | |
| Nodal status | | | | | 0.970 |
| negative | 50 | 55.56 | 11 | 40 | |
| 1 | 33 | 36.67 | 8 | 26 | |
| 2 | 7 | 7.78 | 2 | 3 | |
| Distant metastasis | | | | | 0.259 |
| negative | 86 | 95.56 | 21 | 0 | |
| positive | 4 | 4.44 | 65 | 4 | |
| TNM Stage | | | | | 0.512 |
| I | 3 | 3.33 | 1 | 2 | |
| II | 37 | 41.11 | 6 | 31 | |
| III | 42 | 46.67 | 11 | 31 | |
| IV | 8 | 8.89 | 3 | 5 | |

tissues. A significantly upregulated expression of IFITM1 was found in 76.7% of the patients (69/90), which was consistent with the results analyzed by the microarray data ($p < 0.001$, see **Figures 5A,B**).

Correlation of IFITM1 Expression of Clinical Features in Patients With Pancreatic Cancer

The χ^2 -test was applied to assess the relationship between the expressions of IFITM1 and the clinical and pathologic features

of patients with pancreatic cancer, including gender, age at diagnosis, tumor size, histologic differentiation, TNM stage, nodal status, and distant metastasis. Histologic differentiation ($p = 0.032$) and TNM stage ($p = 0.044$) were found to have close correlations with IFITM1 expression (**Table 3**). Higher expression of IFITM1 correlated with poor histologic differentiation and larger TNM stage. The significant correlation between IFITM1 and the TNM stage was also verified using the GEPIA (<https://www.gepia.cancer-pku.cn>; **Figure 5C**). Consistent with our investigation, IFITM1 might be an oncogene for pancreatic cancer that participates in tumorigenesis.



The Cancer Genome Atlas-Based Analysis Validates the Prognostic IFITM1 Signature

A total of 184 patients with pancreatic cancer in the TCGA database, with 5 of them having no documented T or N stage, leaving 179 patients for the confirmation of the relationship between IFITM1 and human pancreatic cancer. The Kaplan–Meier analysis and the log-rank test were used for analysis. As shown in **Figure 6A**, patients with a low level of IFITM1 had better disease-free survival than those with high IFITM1 (log-rank $p = 0.036$) as well as had a better OS (**Figure 6B**, log-rank $p = 0.014$).

Verification of IFITM1 With Prognostic Signature

For the survival analysis, the median IHC value was used as an objective cutoff to stratify 90 patients with pancreatic cancer with low and high expressions. We used the Kaplan–Meier analysis and the log-rank test to explore the correlation. The follow-up time was 81 months, and a high IFITM1 level was found significantly related to decreased OS ($p = 0.032$; **Figure 6C**). The median OS of the patients with pancreatic cancer with the low and high IFITM1 expression was 43.0 vs. 10.0 months, respectively.

As for the univariable Cox regression analysis, positive nodal status ($p = 0.008$), TNM stage ($p = 0.012$), histologic differentiation ($p = 0.004$), and IFITM1 expression ($p = 0.040$) were significantly associated with worse outcome (**Table 4**). In the multivariable analysis, IFITM1 expression (HR = 2.134; 95% CI 1.073, 4.245; $p = 0.031$) remained an independent prognostic marker for OS of patients with pancreatic cancer (**Table 4**).

Immune Cell Infiltration of IFITM1 in Patients With Pancreatic Cancer

IFN-induced transmembrane protein 1 was found involving in inflammatory processes and immune cells infiltration, which might further influence the clinical outcomes of patients with pancreatic cancer. We used the TIMER database (<https://cistrome.shinyapps.io/timer/>) to explore a comprehensive

relation between IFITM1 levels and immune infiltrations. The positive correlations were assessed between IFITM1 and B cell (Cor = 0.171, $p = 2.51E-2$), CD4+ T cell (Cor = 0.307, $p = 4.90E-5$), macrophage (Cor = 0.204, $p = 7.34E-3$), neutrophil (Cor = 0.475, $p = 5.20E-11$), and dendritic cell (Cor = 0.421, $p = 1.01E-8$). IFITM1 level was in negative association with purity (Cor = -0.165 , $p = 3.1E-2$). Only CD8+ T cell was found having no significant relation to IFITM1 expression (**Figure 7**).

IFN-Induced Transmembrane Protein 1 Silencing Inhibits Tumorigenicity of Pancreatic Cancer

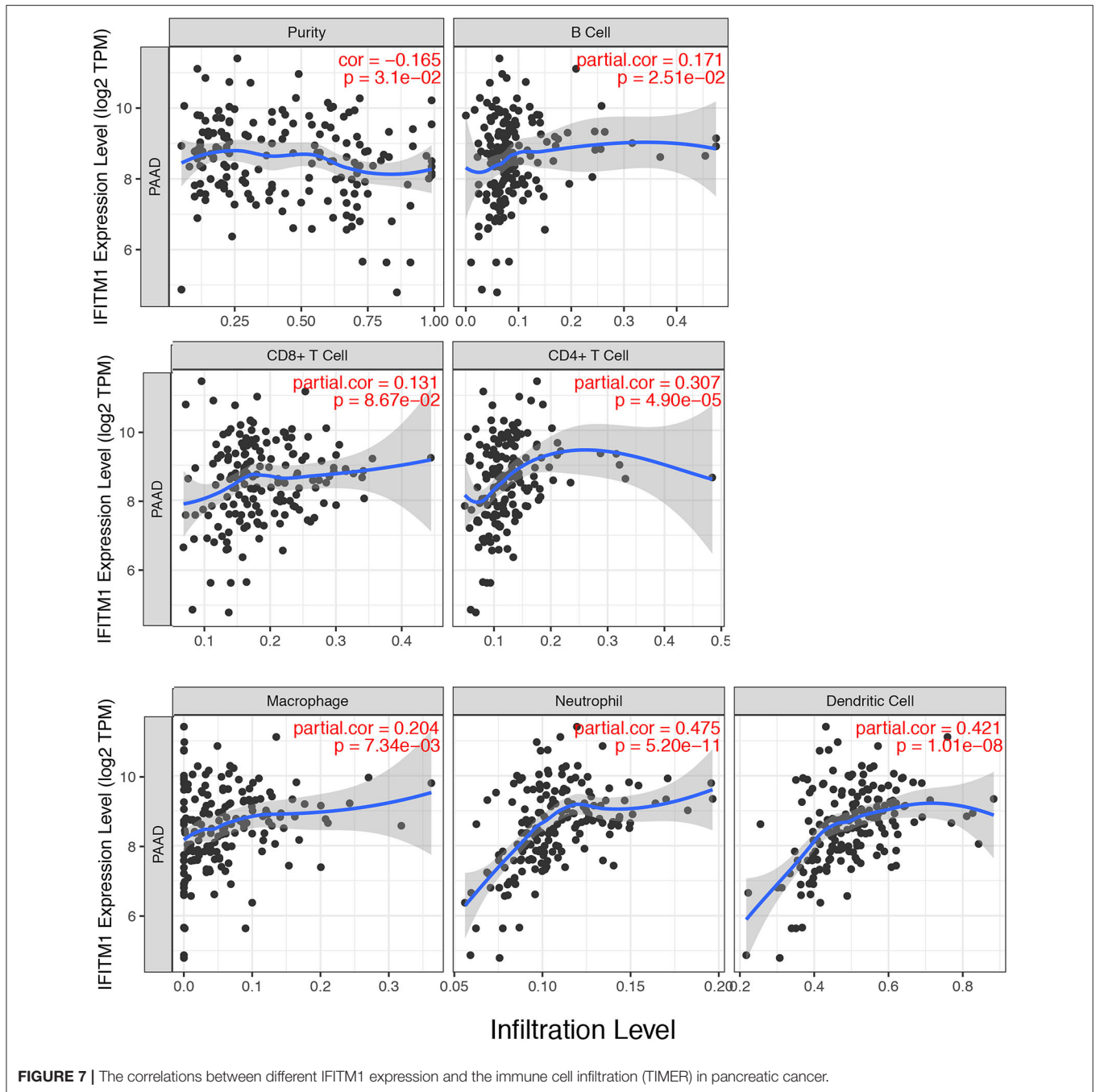
Three types of pancreatic cancer cell lines and normal human pancreatic duct epithelial cell line HPDE6-C7 were used to examine the expressions of IFITM1. As shown in **Figures 8B,C**, higher mRNA and protein levels of IFITM1 were found in BxPc-3, PanC-1, and SW1990 compared to HPDE6-C7. Two shRNA targeting IFITM1 were transfected into PanC-1 and SW1990 to detect the IFITM1 silencing effects, and the efficiency was examined both by qRT-PCR and Western blot analysis (**Figures 8D,E**). We performed cell counting kit-8 assay to assess the cancer cell proliferation. The results showed that the downregulation of IFITM1 significantly decreased the proliferation of PanC-1 and SW1990 cell lines (**Figure 8A**). Moreover, the wound-healing assay indicated that IFITM1 silencing inhibited cell migration capability, and the colony-formation assay showed that it greatly reduced the cancer stem cell-like properties of pancreatic cancer (**Figures 8F-I**).

DISCUSSION

With the highest incidence-to-mortality ratio of solid tumors, pancreatic cancer is an elusive disease seeking explorations to elicit the redundant mechanisms involving pathogenesis, progression, and metastasis. To improve the poor clinical expectations, we identified and verified a potential molecular

TABLE 4 | Univariable and multivariable Cox regression analyses for overall survival, accounting for IFITM1 expression and clinicopathological features in 90 patients with pancreatic cancer.

| Parameter | Univariable | | Multivariable | |
|---|-----------------------|---------|-----------------------|---------|
| | Hazard ratio (95% CI) | p-value | Hazard ratio (95% CI) | p-value |
| Gender (female/male) | 1.164 (0.702, 1.931) | 0.556 | | |
| Age (years; $\leq 65 / > 65$) | 1.200 (0.733, 1.963) | 0.469 | | |
| TNM stage (1/2/3/4) | 1.541 (0.939, 2.529) | 0.087 | | |
| Nodal status (0/1/2) | 1.670 (1.140, 2.447) | 0.008 | 1.026 (0.535, 1.970) | 0.938 |
| Distant metastasis (-/+) | 2.548 (0.921, 7.053) | 0.072 | | |
| TNM Stage (I/II/III/IV) | 1.563 (1.103, 2.215) | 0.012 | 1.684 (0.886, 3.198) | 0.111 |
| Tumor size ($\leq 4.5 / > 4.5$ cm) | 1.212 (0.739, 1.990) | 0.446 | | |
| Histologic differentiation (well/moderately/poorly) | 1.819 (1.214, 2.725) | 0.004 | 1.616 (1.060, 2.462) | 0.026 |
| IFITM1 expression (\leq median/ $>$ median) | 1.971 (1.030, 3.771) | 0.040 | 2.134 (1.073, 4.245) | 0.031 |



biomarker through network-based analytic methods of multiple data sets and etiology-based malignancies characterizing (30).

Systematically, through five microarray gene expression data sets, the FI network-based approach was used to build the functional modules for pancreatic cancer. On the basis of the diverse function of each module, the degree value, and the connectivity of the nodes, IFITM1 was identified as a promising biomarker. Consistent with the outcomes of several bioinformatics online tools, IFITM1 was found highly expressed in pancreatic cancer compared to normal pancreatic tissues and

was confirmed through IHC experiment later. Similarly, previous studies have shown high expressed IFITM1 in a variety of cancers. Through the human cancer profiling array containing 10 samples of lung carcinoma and the corresponding normal samples, IFITM1 was detected increasing significantly in lung carcinoma (40). The difference was also observed in two other studies that demonstrated IFITM1 overexpression through tissues and lung cancer cell lines of patients (8, 41). Immunohistochemistry on TMA of a consecutive cohort including 174 patients with gastroesophageal adenocarcinoma also detected a significant

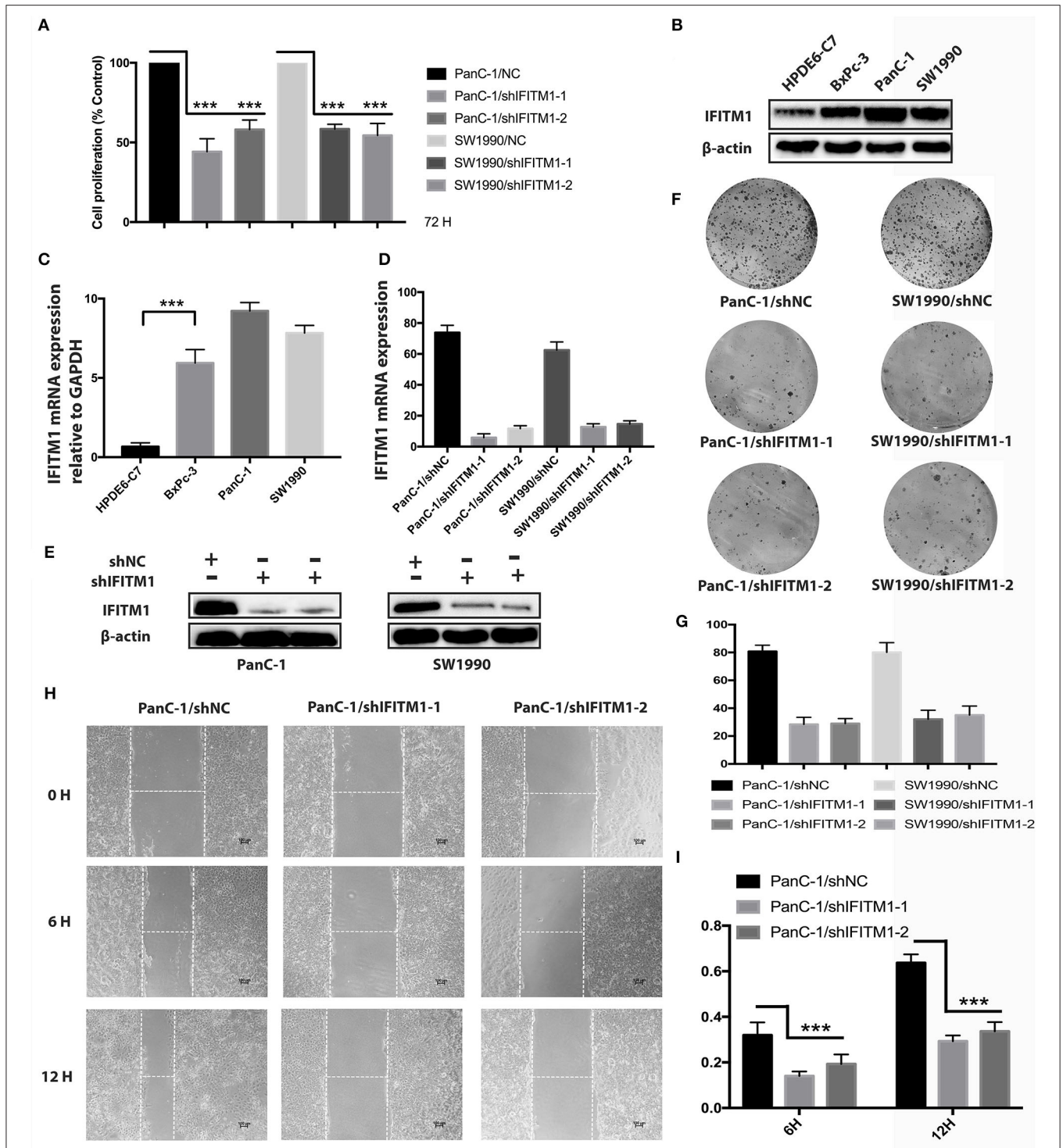


FIGURE 8 | The depletion of IFITM1 decreased the tumorigenicity of pancreatic cancer cells. **(A)** Control (shNC) or IFITM1-depleted (shIFITM1-1 and shIFITM1-2) PanC-1 and SW1990 cell lines were incubated for 72 h to determine the cell proliferation rate by cell counting kit-8 assay. Data represent the mean \pm SD of three independent experiments ($***p < 0.001$). **(B,C)** Detection of IFITM1 mRNA expression in three different pancreatic cancer cell lines and HPDE6-C7 by qRT-PCR and Western blot analysis. GAPDH and β -Actin were used as controls, respectively. The results are expressed as the mean \pm SD of three independent experiments ($***p < 0.001$). **(D,E)** Pancreatic cancer cell lines were transfected with shRNAs (shIFITM1-1 and shIFITM1-2), and the expression level of IFITM1 was assessed by qRT-PCR and Western blot analysis using GAPDH and β -actin as controls, respectively. The results are expressed as mean \pm SD of three independent experiments. **(F,G)** Colony-formation assay was performed to show decreased cancer stem cell-like properties of PanC-1 and SW1990 cells transfected with shIFITM1-1 or shIFITM1-2 compared with control *in vitro*. **(H,I)** The wound-healing assay was performed to assess the effect of IFITM1 silencing on the wound closure ability of PanC-1 cells. Representative images are shown (magnification $\times 100$).

elevation of IFITM1 in primary tumors along with lymph node metastases, compared to the adjacent normal epithelium and intestinal metaplasia (42). Gastric cancer samples derived from 27 patients and 6 gastric cancer cell lines, and tissues of 4 patients and 4 tumor cell lines were assessed by Lee et al. (7) and Yang et al. (43) separately and showed the same findings. Moreover, aberrant expressions of IFITM1 detected through cancer array profiling, immunohistochemistry, RT-PCR, immunoblotting, and immunofluorescence analysis were verified in colorectal cancer, hepatocellular carcinoma, head and neck squamous cell carcinoma (HNSCC), gallbladder, and ovarian cancer (6, 8, 23, 44–46).

Notably, the histologic differentiation ($p = 0.032$) and TNM stage ($p = 0.044$) of the patients with pancreatic cancer were significantly correlated with IFITM1 expression in the clinical and pathological analyses. In order to explore the underlining mechanisms, we found the role of IFITM1 has been shown in the tumorigenesis involving tumor cells unlimited proliferation, invasion, angiogenesis, metastasis, and treatment resistance. Overexpression of IFITM1 was for the first time found to enhance cancer migration and invasion in 2005, with the cell model of gastric cancer (43). The phenomenon was then discovered in HNSCC, glioma, and gastric cells *in vitro* experiments, and meanwhile the downregulation of IFITM1 significantly decreased the activity of matrix metalloproteinase 9 (MMP9) (44, 47). Two studies revealed that the depletion of IFITM1 significantly inhibited aromatase inhibitor (AI)-resistant breast cancer growth, and the invasion and observation reversed with the ectopic level of IFITM1 (48, 49). Recently, Yang et al. (43) demonstrated that IFITM1 was essentially required for the progression of non-small cell lung cancer (NSCLC), both *in vitro* and *in vivo* and the silenced expression of IFITM1 significantly reduced the capacity of sphere-formation, invasion, and migration of NSCLC.

To further validate the prognostic signature of IFITM1 in patients with pancreatic cancer, both univariable and multivariable Cox regression analyses were assessed, and the data suggested IFITM1 as an independent prognostic marker. Similar prognostic values were also seen in other types of tumors (42, 45, 50). Chemotherapy, radiation therapy, and endocrine therapy are three critical and effective strategies in cancer treatment. Accumulating evidence has indicated that IFITM1 was involved in radio- and chemo-resistance as well as endocrine therapy resistance. In our previous study, we explored the radiosensitive possibility of adipose-derived mesenchymal stem cells and discovered IFITM1 could be an important target involved in radioresistance (23). Mechanically, the upregulation level of IFITM1 was correlated with high expression of STAT3 and MMP family and also with the downregulation of P53 and caspase family. The association between IFITM1 and signal transducer STAT at the molecular level was also detected and evaluated by knockdown of IFITM1 in oral tumors (51, 52). While the interaction between IFITM1 and P53 signaling cascades, the apoptotic effects of other IFITM proteins were mainly P53-independent (53). Yet, it is still unclear whether IFITM1 is of prime importance in the responsiveness of patients with pancreatic cancer to clinical therapies.

In addition to the multiple cell functions involving anti-proliferation and adhesion, the IFITM1 is predominantly important in immune responses (54). As we discovered above, immune cell infiltration was in significant correlation with IFITM1 in pancreatic cancer. Escape of natural killer cell recognition was reported from gastric cancer cells with an increased level of IFITM1 (43). This indicated that tumors expressing high IFITM1 were insensitive to the antiproliferative therapies, which might be attributed to escaping immune surveillance.

Although we discovered the potential role of IFITM1 in pancreatic cancer, limitations to this study were acknowledged. A tumor xenograft model is needed to verify the outcomes *in vivo* experiments, and a larger cohort of patients with pancreatic cancer are expected to validate the data.

Taken together, our study constructed an effective FI network-based module analysis to discover the differentially expressed genes between pancreatic cancer and normal pancreatic tissues and suggested that the upregulation of IFITM1 correlated to a poor clinical result of pancreatic cancer.

DATA AVAILABILITY STATEMENT

The original contributions presented in the study are included in the article/**Supplementary Material**, further inquiries can be directed to the corresponding author/s.

ETHICS STATEMENT

The studies involving human participants were reviewed and approved by the Ethical Committees of the National Engineering Center for Biochips at Alenabio and Shanghai Outdo Biotech Company and Taizhou People's Hospitals. The patients/participants provided their written informed consent to participate in this study. The animal study was reviewed and approved by the Ethical Committees of the National Engineering Center for Biochips at Alenabio and Shanghai Outdo Biotech Company and Taizhou People's Hospitals. Written informed consent was obtained from the individual(s) for the publication of any potentially identifiable images or data included in this article.

AUTHOR CONTRIBUTIONS

SY and CM were responsible for the research design and participated in the paper. LW and XZ drafted the manuscript and participated in data collection and analysis. LW, XZ, MT, and DY performed the laboratory experiments. All authors were responsible for data analysis and figure format.

FUNDING

This study was supported by grants from the Chinese Medicine Research Program of Zhejiang Province (Grant No.2018ZZ014)

and the Zhejiang Provincial key Discipline of Traditional Chinese Medicine (Grant No.2017-XX-A32).

ACKNOWLEDGMENTS

The authors thank Professor Chen Xin (Zhejiang University School of Medicine, Hangzhou, China) for the professional support and help, and Mr. Cui Jinlong (Zhejiang University

School of Medicine, Hangzhou, China) for the professional assistance in tissue staining valuation.

SUPPLEMENTARY MATERIAL

The Supplementary Material for this article can be found online at: <https://www.frontiersin.org/articles/10.3389/fonc.2021.626883/full#supplementary-material>

REFERENCES

- Rahib L, Smith BD, Aizenberg R, Rosenzweig AB, Fleshman JM, Matrisian LM. Projecting cancer incidence and deaths to 2030: the unexpected burden of thyroid, liver, and pancreas cancers in the United States. *Cancer Res.* (2014) 74:2913–21. doi: 10.1158/0008-5472.CAN-14-0155
- Robin F, Angenard G, Cano L, Courtin-Tanguy L, Gaignard E, Khene ZE, et al. Molecular profiling of stroma highlights stratifin as a novel biomarker of poor prognosis in pancreatic ductal adenocarcinoma. *Br J Cancer.* (2020) 123:72–80. doi: 10.1038/s41416-020-0863-1
- Christenson ES, Jaffee E, Azad NS. Current and emerging therapies for patients with advanced pancreatic ductal adenocarcinoma: a bright future. *Lancet Oncol.* (2020) 21:e135–45. doi: 10.1016/S1470-2045(19)30795-8
- Diamond MS, Farzan M. The broad-spectrum antiviral functions of IFIT and IFITM proteins. *Nat Rev Immunol.* (2013) 13:46–57. doi: 10.1038/nri3344
- Friedman RL, Manly SP, McMahon M, Kerr IM, Stark GR. Transcriptional and posttranscriptional regulation of interferon-induced gene expression in human cells. *Cell.* (1984) 38:745–55. doi: 10.1016/0092-8674(84)90270-8
- Kim NH, Sung HY, Choi EN, Lyu D, Choi HJ, Ju W, et al. Aberrant DNA methylation in the IFITM1 promoter enhances the metastatic phenotype in an intraperitoneal xenograft model of human ovarian cancer. *Oncol Rep.* (2014) 31:2139–46. doi: 10.3892/or.2014.3110
- Lee J, Goh SH, Song N, Hwang JA, Nam S, Choi IJ, et al. Overexpression of IFITM1 has clinicopathologic effects on gastric cancer and is regulated by an epigenetic mechanism. *Am J Pathol.* (2012) 181:43–52. doi: 10.1016/j.ajpath.2012.03.027
- Yang YG, Koh YW, Sari IN, Jun N, Lee S, Phi LTH, et al. Interferon-induced transmembrane protein 1-mediated EGFR/SOX2 signaling axis is essential for progression of non-small cell lung cancer. *Int J Cancer.* (2019) 144:2020–32. doi: 10.1002/ijc.31926
- Yu F, Xie D, Ng SS, Lum CT, Cai MY, Cheung WK, et al. IFITM1 promotes the metastasis of human colorectal cancer via CAV-1. *Cancer Lett.* (2015) 368:135–43. doi: 10.1016/j.canlet.2015.07.034
- Ramanathan A, Ramanathan A. Interferon induced transmembrane Protein-1 gene expression as a biomarker for early detection of invasive potential of oral squamous cell carcinomas. *Asian Pac J Cancer Prev.* (2016) 17:2297–9. doi: 10.7314/APJCP.2016.17.4.2297
- Sari IN, Yang YG, Phi LT, Kim H, Baek MJ, Jeong D, et al. Interferon-induced transmembrane protein 1 (IFITM1) is required for the progression of colorectal cancer. *Oncotarget.* (2016) 7:86039–50. doi: 10.18632/oncotarget.13325
- Wright GW, Simon RM. A random variance model for detection of differential gene expression in small microarray experiments. *Bioinformatics.* (2003) 19:2448–55. doi: 10.1093/bioinformatics/btg345
- Pathan M, Keerthikumar S, Ang CS, Gangoda L, Quek CY, Williamson NA, et al. FunRich: an open access standalone functional enrichment and interaction network analysis tool. *Proteomics.* (2015) 15:2597–601. doi: 10.1002/pmic.201400515
- Niu X, Zhang J, Ni J, Wang R, Zhang W, Sun S, et al. Network pharmacology-based identification of major component of *Angelica sinensis* and its action mechanism for the treatment of acute myocardial infarction. *Biosci Rep.* (2018) 38:BSR20180519. doi: 10.1042/BSR20180519
- Akey JM, Biswas S, Leek JT, Storey JD. On the design and analysis of gene expression studies in human populations. *Nat Genet.* (2007) 39:807–8; author reply 808–9. doi: 10.1038/ng0707-807
- Croft D, O'Kelly G, Wu G, Haw R, Gillespie M, Matthews L, et al. Reactome: a database of reactions, pathways and biological processes. *Nucleic Acids Res.* (2011) 39:D691–7. doi: 10.1093/nar/gkq1018
- Shannon P, Markiel A, Ozier O, Baliga NS, Wang JT, Ramage D, et al. Cytoscape: a software environment for integrated models of biomolecular interaction networks. *Genome Res.* (2003) 13:2498–504. doi: 10.1101/gr.1239303
- Wu G, Dawson E, Duong A, Haw R, Stein L. ReactomeFIViz: a Cytoscape app for pathway and network-based data analysis. *F1000Res.* (2014) 3:146. doi: 10.12688/f1000research.4431.2
- Zhao X, Xu M, Cai Z, Yuan W, Cui W, Li MD. Identification of LIFR, PIK3R1, and MMP12 as novel prognostic signatures in gallbladder cancer using network-based module analysis. *Front Oncol.* (2019) 9:325. doi: 10.3389/fonc.2019.00325
- Uhlen M, Fagerberg L, Hallstrom BM, Lindskog C, Oksvold P, Mardinoglu A, et al. Proteomics. tissue-based map of the human proteome. *Science.* (2015) 347:1260419. doi: 10.1126/science.1260419
- Rhodes DR, Yu J, Shanker K, Deshpande N, Varambally R, Ghosh D, et al. ONCOMINE: a cancer microarray database and integrated data-mining platform. *Neoplasia.* (2004) 6:1–6. doi: 10.1016/S1476-5586(04)80047-2
- Tang Z, Li C, Kang B, Gao G, Li C, Zhang Z. GEPIA: a web server for cancer and normal gene expression profiling and interactive analyses. *Nucleic Acids Res.* (2017) 45:W98–102. doi: 10.1093/nar/gkx247
- Wu L, Tang Q, Yin X, Yan D, Tang M, Xin J, et al. The therapeutic potential of adipose tissue-derived mesenchymal stem cells to enhance radiotherapy effects on hepatocellular carcinoma. *Front Cell Dev Biol.* (2019) 7:267. doi: 10.3389/fcell.2019.00267
- Keshava Prasad TS, Goel R, Kandasamy K, Keerthikumar S, Kumar S, Mathivanan S, et al. Human protein reference database—2009 update. *Nucleic Acids Res.* (2009) 37:D767–72. doi: 10.1093/nar/gkn892
- Chatr-Aryamontri A, Breitkreutz BJ, Oughtred R, Boucher L, Heinicke S, Chen D, et al. The BioGRID interaction database: 2015 update. *Nucleic Acids Res.* (2015) 43:D470–8. doi: 10.1093/nar/gku1204
- Brown KR, Jurisica I. Unequal evolutionary conservation of human protein interactions in interologous networks. *Genome Biol.* (2007) 8:R95. doi: 10.1186/gb-2007-8-5-r95
- Orchard S, Ammari M, Aranda B, Breuza L, Briganti L, Broackes-Carter F, et al. The MIntAct project—IntAct as a common curation platform for 11 molecular interaction databases. *Nucleic Acids Res.* (2014) 42:D358–63. doi: 10.1093/nar/gkt1115
- Licata L, Briganti L, Peluso D, Perfetto L, Iannuccelli M, Galeota E, et al. MINT, the molecular interaction database: 2012 update. *Nucleic Acids Res.* (2012) 40:D857–61. doi: 10.1093/nar/gkr930
- Salwinski L, Miller CS, Smith AJ, Pettit FK, Bowie JU, Eisenberg D. The database of interacting proteins: 2004 update. *Nucleic Acids Res.* (2004) 32:D449–51. doi: 10.1093/nar/gkh086
- Wu G, Feng X, Stein L. A human functional protein interaction network and its application to cancer data analysis. *Genome Biol.* (2010) 11:R53. doi: 10.1186/gb-2010-11-5-r53
- Masoudi S, Hassanzadeh Nemati A, Fazli HR, Beygi S, Moradzadeh M, Pourshams A, et al. An increased level of aryl hydrocarbon receptor in patients with pancreatic cancer. *Middle East J Dig Dis.* (2019) 11:38–44. doi: 10.15171/mejdd.2018.126
- Segara D, Biankin AV, Kench JG, Langusch CC, Dawson AC, Skalicky DA, et al. Expression of HOXB2, a retinoic acid signaling target in pancreatic

- cancer and pancreatic intraepithelial neoplasia. *Clin Cancer Res.* (2005) 11:3587–96. doi: 10.1158/1078-0432.CCR-04-1813
33. Badea L, Herlea V, Dima SO, Dumitrascu T, Popescu I. Combined gene expression analysis of whole-tissue and microdissected pancreatic ductal adenocarcinoma identifies genes specifically overexpressed in tumor epithelia. *Hepatogastroenterology.* (2008) 55:2016–27.
 34. Logsdon CD, Simeone DM, Binkley C, Arumugam T, Greenson JK, Giordano TJ, et al. Molecular profiling of pancreatic adenocarcinoma and chronic pancreatitis identifies multiple genes differentially regulated in pancreatic cancer. *Cancer Res.* (2003) 63:2649–57.
 35. Ishikawa M, Yoshida K, Yamashita Y, Ota J, Takada S, Kisanuki H, et al. Experimental trial for diagnosis of pancreatic ductal carcinoma based on gene expression profiles of pancreatic ductal cells. *Cancer Sci.* (2005) 96:387–93. doi: 10.1111/j.1349-7006.2005.00064.x
 36. Iacobuzio-Donahue CA, Maitra A, Olsen M, Lowe AW, van Heek NT, Rosty C, et al. Exploration of global gene expression patterns in pancreatic adenocarcinoma using cDNA microarrays. *Am J Pathol.* (2003) 162:1151–62. doi: 10.1016/S0002-9440(10)63911-9
 37. Buchholz M, Braun M, Heidenblut A, Kestler HA, Kloppel G, Schmiegel W, et al. Transcriptome analysis of microdissected pancreatic intraepithelial neoplastic lesions. *Oncogene.* (2005) 24:6626–36. doi: 10.1038/sj.onc.1208804
 38. Grutzmann R, Pilarsky C, Ammerpohl O, Luttges J, Bohme A, Sipos B, et al. Gene expression profiling of microdissected pancreatic ductal carcinomas using high-density DNA microarrays. *Neoplasia.* (2004) 6:611–22. doi: 10.1593/neo.04295
 39. Pei H, Li L, Fridley BL, Jenkins GD, Kalari KR, Lingle W, et al. FKBP51 affects cancer cell response to chemotherapy by negatively regulating Akt. *Cancer Cell.* (2009) 16:259–66. doi: 10.1016/j.ccr.2009.07.016
 40. Andreu P, Colnot S, Godard C, Laurent-Puig P, Lamarque D, Kahn A, et al. Identification of the IFITM family as a new molecular marker in human colorectal tumors. *Cancer Res.* (2006) 66:1949–55. doi: 10.1158/0008-5472.CAN-05-2731
 41. Yan J, Jiang Y, Lu J, Wu J, Zhang M. Inhibiting of proliferation, migration, and invasion in lung cancer induced by silencing Interferon-Induced Transmembrane Protein 1 (IFITM1). *Biomed Res Int.* (2019) 2019:9085435. doi: 10.1155/2019/9085435
 42. Borg D, Hedner C, Gaber A, Nodin B, Fristedt R, Jirstrom K, et al. Expression of IFITM1 as a prognostic biomarker in resected gastric and esophageal adenocarcinoma. *Biomark Res.* (2016) 4:10. doi: 10.1186/s40364-016-0064-5
 43. Yang Y, Lee JH, Kim KY, Song HK, Kim JK, Yoon SR, et al. The interferon-inducible 9-27 gene modulates the susceptibility to natural killer cells and the invasiveness of gastric cancer cells. *Cancer Lett.* (2005) 221:191–200. doi: 10.1016/j.canlet.2004.08.022
 44. Hatano H, Kudo Y, Ogawa I, Tsunematsu T, Kikuchi A, Abiko Y, et al. IFN-induced transmembrane protein 1 promotes invasion at early stage of head and neck cancer progression. *Clin Cancer Res.* (2008) 14:6097–105. doi: 10.1158/1078-0432.CCR-07-4761
 45. He J, Li J, Feng W, Chen L, Yang K. Prognostic significance of INF-induced transmembrane protein 1 in colorectal cancer. *Int J Clin Exp Pathol.* (2015) 8:16007–13.
 46. Li D, Yang Z, Liu Z, Zou Q, Yuan Y. DDR2 and IFITM1 are prognostic markers in gallbladder squamous cell/adenosquamous carcinomas and adenocarcinomas. *Pathol Oncol Res.* (2019) 25:157–67. doi: 10.1007/s12253-017-0314-3
 47. Gonzalez-Avila G, Sommer B, Mendoza-Posada DA, Ramos C, Garcia-Hernandez AA, Falfan-Valencia R. Matrix metalloproteinases participation in the metastatic process and their diagnostic and therapeutic applications in cancer. *Crit Rev Oncol Hematol.* (2019) 137:57–83. doi: 10.1016/j.critrevonc.2019.02.010
 48. Choi HJ, Lui A, Ogony J, Jan R, Sims PJ, Lewis-Wambi J. Targeting interferon response genes sensitizes aromatase inhibitor resistant breast cancer cells to estrogen-induced cell death. *Breast Cancer Res.* (2015) 17:6. doi: 10.1186/s13058-014-0506-7
 49. Lui AJ, Geanes ES, Ogony J, Behbod F, Marquess J, Valdez K, et al. IFITM1 suppression blocks proliferation and invasion of aromatase inhibitor-resistant breast cancer *in vivo* by JAK/STAT-mediated induction of p21. *Cancer Lett.* (2017) 399:29–43. doi: 10.1016/j.canlet.2017.04.005
 50. Balbous A, Cortes U, Guilloteau K, Villalva C, Flamant S, Gaillard A, et al. A mesenchymal glioma stem cell profile is related to clinical outcome. *Oncogenesis.* (2014) 3:e91. doi: 10.1038/oncsis.2014.5
 51. Liang R, Li X, Zhu X. Deciphering the roles of IFITM1 in tumors. *Mol Diagn Ther.* (2020) 24:433–41. doi: 10.1007/s40291-020-00469-4
 52. Yang J, Li L, Xi Y, Sun R, Wang H, Ren Y, et al. Combination of IFITM1 knockdown and radiotherapy inhibits the growth of oral cancer. *Cancer Sci.* (2018) 109:3115–28. doi: 10.1111/cas.13640
 53. Xu Y, Yang G, Hu G. Binding of IFITM1 enhances the inhibiting effect of caveolin-1 on ERK activation. *Acta Biochim Biophys Sin.* (2009) 41:488–94. doi: 10.1093/abbs/gmp034
 54. Siegrist F, Ebeling M, Certa U. The small interferon-induced transmembrane genes and proteins. *J Interferon Cytokine Res.* (2011) 31:183–97. doi: 10.1089/jir.2010.0112

Conflict of Interest: The authors declare that the research was conducted in the absence of any commercial or financial relationships that could be construed as a potential conflict of interest.

Copyright © 2021 Wu, Zhu, Yan, Tang, Ma and Yan. This is an open-access article distributed under the terms of the Creative Commons Attribution License (CC BY). The use, distribution or reproduction in other forums is permitted, provided the original author(s) and the copyright owner(s) are credited and that the original publication in this journal is cited, in accordance with accepted academic practice. No use, distribution or reproduction is permitted which does not comply with these terms.